Open Access
Check for updates
International Journal of Medical Science and Dental Health (ISSN: 2454-4191)
Volume 11, Issue 11, November 2025
Doi: https://doi.org/10.55640/ijmsdh-11-11-12

# Synthesis and Characterization of $Mn_2O_3$/Cuo Nanocomposite Using A Spirulina Biological Model for Dye Degradation in Polluted Water Under Visible Light

**ZAHRAA KAMIL SALMAN**
Directorate General of Education, Ministry of Education, Karbala, Iraq.

**Received:** 20 October 2025, **accepted:** 27 October 2025, **Published Date:** 17 November 2025

## Abstract

The release of pollutants into the environment has increased significantly as a result of the widespread use of paints in various industries. The reactive black 5 (RB-5) is one of the most popular azo-based dyes, it's also one of the most commonly used synthetic dyes in the textile industry because of its azo group (N=N). Since this chemical is toxic and has a severe impact on the environment, it's essential to eliminate it from the environment. The objective of this research was to create and characterize Mn2O3-CuO nanocomposites using extracts from Spirulina, then utilize them to degrade the color of the dye RB5 in polluted water. Mn2O3 nanoparticles were created by the coprecipitation method, then copper oxide was created using Spirulina's extracts in conjunction with Mn2O3 nanoparticles. The resultant Mn2O3-CuO nanocomposites were then studied by X-ray diffraction (XRD), field emission scanning electron microscopy (FESEM), and energy dispersive X-ray analysis (EDX). Under the most beneficial conditions, the pH was 5, the amount of Mn2O3-CuO was 40 mg, and 120 minutes of lightning had a greater than 90% removal of the color from the water sample. Additionally, the composed nanomaterial could be utilized for at least four cycles without a significant loss of its photocatalytic capabilities.

**Keywords:** Reactive Black 5 (RB-5), Mn2O3-CuO nanocomposite, Photocatalyst

## 1. Introduction

Increased chemical production in numerous sectors, combined with a fast-rising population, has increased worldwide water contamination. Wastewater created by the textile, leather, pharmaceutical, and paper sectors is commonly polluted with a variety of colours. Textile manufacture is a major contributor to dye pollution, since even modest dye concentrations (less than 1 ppm) may substantially degrade the transparency, gas solubility, and general cleanliness of rivers, lakes, and other water bodies [1, 2]. Azo dyes include nitrogen double bonds (N=N) in their chemical structure and account for more than 70% of the worldwide dye industry. They are extensively employed as reactive dyes. The brilliant colors of wastewater not only impact aesthetics, but also harm the ecosystem and human health [3]. Reactive Black 5 (RB5) is a synthetic reactive azo dye commonly used in the textile industry for fabric dyeing. RB5 is of special concern because of its toxicity, mutagenicity, low biodegradability, and possible carcinogenicity [4]. Therefore, minimising or eliminating the discharge of colored wastewater is crucial for environmental conservation and public health. Conventional procedures such as adsorption[5-9], filtration[10, 11], biodegradation[12] and coagulation[13, 14] have been utilised to remediate dye-contaminated water. However, the chemical stability of dyes often limits the effectiveness of these treatments and leads to challenges such as high cost, incomplete degradation of pollutants and the mere transformation

of pollutants from liquid to solid phase, resulting in secondary wastes that require further treatment. In contrast, photocatalysis has developed as an efficient approach for dye degradation in recent decades [15, 16]. In particular, photocatalytic oxidation technology has garnered considerable interest because to its capacity to effectively mineralize a range of contaminants utilising sustainable solar energy and the added benefit of photocatalyst recycling and regeneration. The photocatalytic degradation pathway contains many essential steps: (1) Photon absorption and electron excitation: When a semiconductor photocatalyst is subjected to incoming light with sufficient energy (hv), it absorbs radiation, causing electrons in the valence band ($e^-$) to be excited and migrate to the conduction band. This process leaves behind positively charged vacancies, so-called photogenerated holes ($h^+$). (2) Redox reactions and production of reactive oxygen species (ROS): Excited electrons and holes engage in redox reactions at their respective energy levels. In the conduction band, electrons ($e^-$) combine with oxygen ($O_2$) to create superoxide radicals ($O_2\bullet^-$). At the same time, photogenerated holes ($h^+$) in the valence band combine with hydroxide ions ($OH^-$) or water molecules to make hydroxyl radicals (•OH). (3) Pollutant degradation: Reactive radicals (•OH, $O_2\bullet^-$) and photogenerated holes ($h^+$) are potent oxidants that engage with pollutant molecules and degrade their chemical structures into less hazardous oxidation products [16]. Among many metal oxides, copper oxide (CuO) has gained extensive interest owing to its exceptional features as a p-type semiconductor (band gap of 1.2 to 2.0 eV) [17]. The monoclinic structure of CuO shows exceptional physical and chemical characteristics, including outstanding thermal stability, electrical conductivity, and redox potential. Its structure comprises of 3d and O2p orbitals that contribute to the conduction band (CB) and valence band (VB) edges, resulting in a narrow band gap that promotes the maximal production of reactive oxygen species (ROS) [18]. CuO photocatalysts not only have a high redox potential, but also can efficiently release OH and $O_2$ radicals, which are critical for photodegradation [19]. CuO nanoparticles (NPs) have been produced utilising several chemical and physical approaches [20]. Among these, green synthesis is a basic, ecologically friendly process that generally employs plants or microorganisms to accomplish non-toxic and sustainable manufacturing. A famous example is Spirulina, a member of the blue-green microalgae (cyanobacteria) family that is prevalent in tropical and subtropical lakes with high carbonate and bicarbonate levels. [21]. Recently, this alga has been exploited for the biosynthesis of metal nanoparticles such as silver and gold [22, 23]. The purpose of the proposed research project is to manufacture $Mn_2O_3$-CuO nanocomposites and assess their efficacy in the photocatalytic degradation of RB5. Field emission scanning electron microscopy (FESEM), energy dispersive X-ray analysis (EDX), and X-ray diffraction (XRD) were then utilised to characterize the produced nanocomposites and establish the best conditions.

## 2. Experimental

### 2.1. Instruments

The concentration of the RB5 dye was determined using a 2100 UNICO single-beam ultraviolet-visible spectrophotometer (China). The ultraviolet-visible spectrum was recorded with a 1 cm wide quartz cell. The pH of the solution was recorded using a digital pH meter that is Switzerland-owned: the 827 model. The shape and composition of the adsorbent were confirmed using a TESCAN BRNO-Mira3 LMU field emission microscope (FESEM) with an EDX system, and X-ray diffraction analysis was conducted using a D8 Bruker device (U.S.A). The adsorbent was separated from the sample solution by using a centrifuge (Andreas Hettich D72, Germany).

### 2.2. Chemicals

The Dye RB5 (Merck, Germany) was made in deionized water at a concentration of 1000 mg/l. More dilute solutions are possible by reducing the concentration of the stock solution. Manganese chloride tetrahydrate ($MnCl_2{\cdot}4H_2O$, 99.0%), ethylenediaminetetraacetic acid (EDTA, 99.5%), and copper sulfate pentahydrate ($CuSO_4{\cdot}5H_2O$, 99.5%) were purchased from Merck, Germany. The solution's pH was altered using a mixture of nitric and sodium hydroxide that was Dilute (0.1 mol/l)..

### 2.3. Synthesis of nanomaterial

#### 2.3.1. Preparation of Spirulina algae extract

The dried Spirulina was preserved in a plastic container and then ground it into a small powder using a mill. Around 10 g of algae powder was incorporated into 100 ml of deionized water in a conical vessel and the mixture was heated to 75 degrees Celsius for 20 minutes in order

to release the chemical compounds present in the algae. The extract was subsequently refrigerated and passed through Whatman paper to be filtered. The final extract was employed to create CuO NPs..

### 2.3.2. Synthesis of $Mn_2O_3$ NPs

$Mn_2O_3$ nanoparticles were created by the coprecipitation method. The solution with 0.2 mol/l of MnCl2.4$H_2O$ and EDTA was made in deionized water. 4 parts per 10,000 of NaOH were added to the solution in small quantities until the pH reached 12. The solution was then stirred at 70 degrees Celsius for 2 hours, the resulting precipitate was then collected by centrifugation and washed three times with deionized water. The manufactured nanoparticles were dried at 90°C for 24 hours and then heated in an oven at 550°C for 6 hours. The manufactured NPs of Mn were used to create MnO-CuO nanocomposites.

### 2.3.3. Synthesis of $Mn_2O_3$-CuO nanocomposite

To create the Mn2O3-CuO composite, the previously prepared Mn2O3 NPs were first sonicated in 50 ml of distilled water. Later, 10 ml of a solution with a concentration of 0.5 mol/l CuSO4.5H2O was added to the mixture and stirred for 10 minutes. Next, 20 ml of Spirulina's extract was added to the mixture and stirred for another 3 hours. After this, the resulting Mn2O3-CuO composite precipitate was separated by centrifugation at 6000 rpm and then washed three times with deionized water. Ultimately, it was placed in an oven at 500 degrees Celsius for 3 hours and dried out and heated to create the Mn2O3-CuO composite.

### 2.3.4. Photocatalyst degradation procedure

Photocatalytic experiments were conducted to investigate the deterioration of the pollutant RB5 in water. A 300-watt xenon lamp that was located in a cylindrical trap made of quartz was employed as the sole light source for the solar system. For this endeavor, 30 ml of the RB5 solution was placed in a dual-walled flasks and different amounts of photocatalyzer were added to the solution. During the experiment, the aqueous solution with RB5 and the prepared nanostructures was stirred at a temperature of 25 °C. Photocatalytic experiments were conducted at different concentrations of pollutant and at different pH values between 3 and 9 in order to determine the effect of the sample's pH and RB5 concentration on the catalytic ability of the prepared photocatalyst. After a designated amount of time with the light source, 5 ml of the suspension was collected and after centrifugation to separate the photocatalyst particles, its absorbance was measured at a specific wavelength of 599nm using a UNICO 2100 UV spectrophotometer. The percentage of the pollutants that were degraded by the photocatalytic process was determined using the following formula.

$$\textbf{Removal Efficiency} = \frac{C_O - C_e}{C_O} \times 100$$

**Equation 1**

## 3. Results and Discussion

### 3.1. Characterization of $Mn_2O_3$-CuO nanocomposite

XRD is a powerful technique for determining the crystal structure. The X-ray spectrum of Mn2O3 particles is demonstrated in Figure 1. The results demonstrate that the peaks at 2θ values of 22.5, 32.6, 39.0, 44.9, 49.0, 54.0, and 65.5 correspond to (121), (222), (004), (332), (341), (404), (161) and (226) phases, respectively, indicating that orthorhombic Mn2O3 particles (JCPDS card 73-1826) were successfully produced [24, 25]. Also depicted in figure 2 is the XRD spectrum of the Mn2O3-CuO composite. The results demonstrate that the peaks of CuO are at 2θ values of 35.5, 39.0, 49.0, 65.5 and 67.5, which correspond to the (111), (200), (-202), (022) and (113) planes, respectively. This indicates that CuO is present in the material's composition [26, 27].

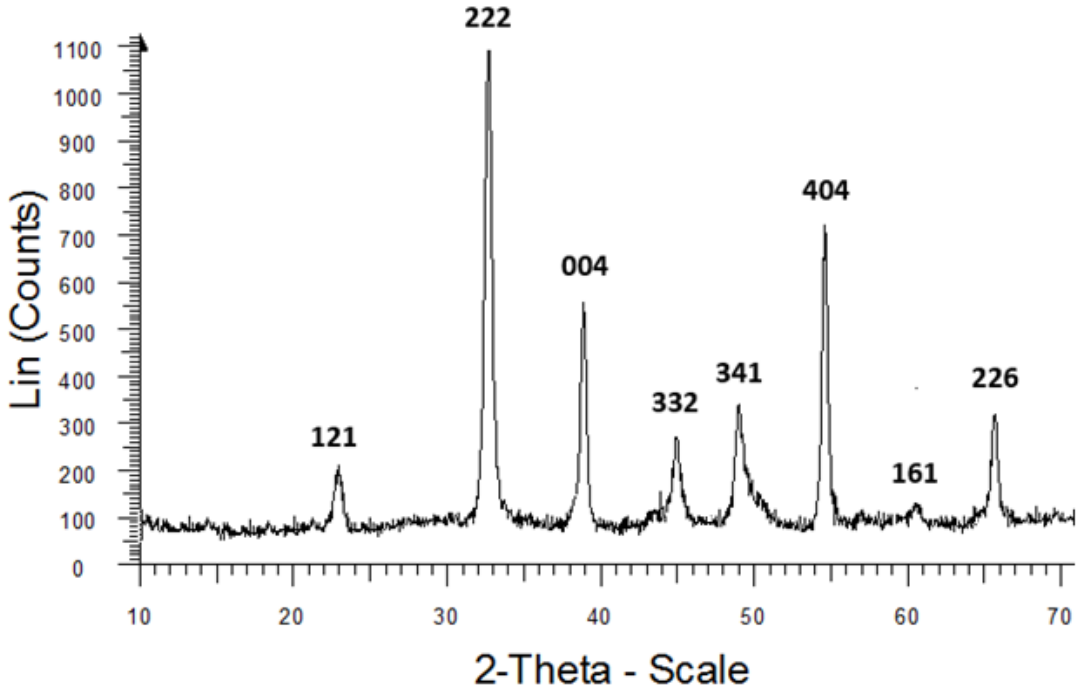


**Fig. 1. XRD spectrum of the synthesized $Mn_2O_3$ NPs**

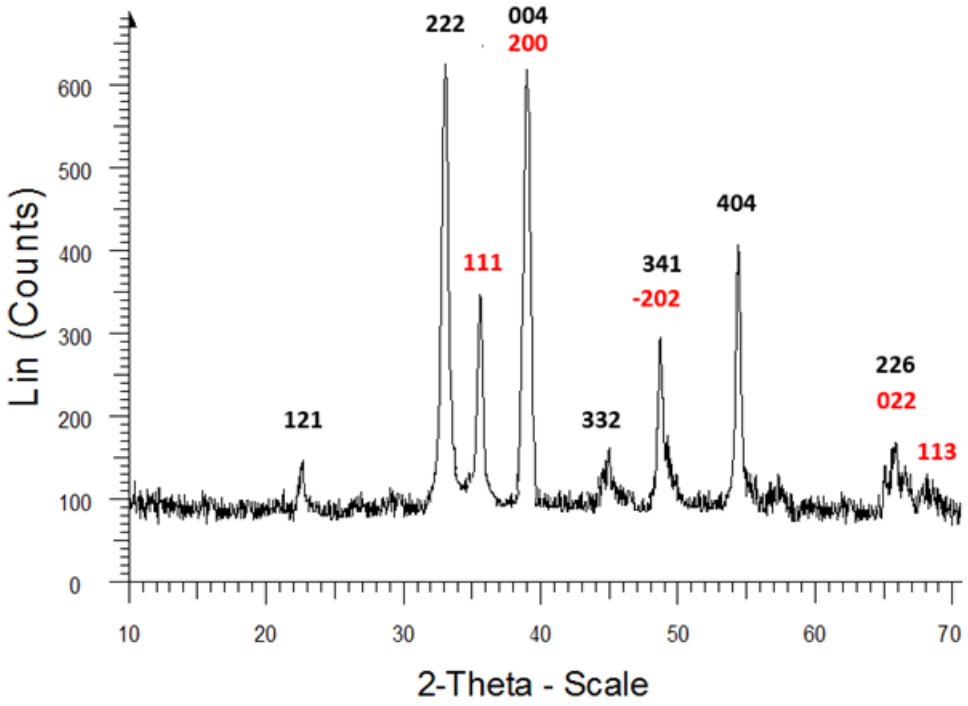


**Fig. 2. XRD spectrum of the synthesized CuO-$Mn_2O_3$ nanocomposite**

Figure 3(a, b) depicts the FESEM images of the manufactured $Mn_2O_3$ NPs and $Mn_2O_3$-CuO composites. The results indicate that the size of Mn2O3 NPs is around 100nm (Figure 3a). However, after the Mn2O3 NPs were converted into CuO NPs using a green-based method, their shape was completely altered, as demonstrated in Figure 3b.

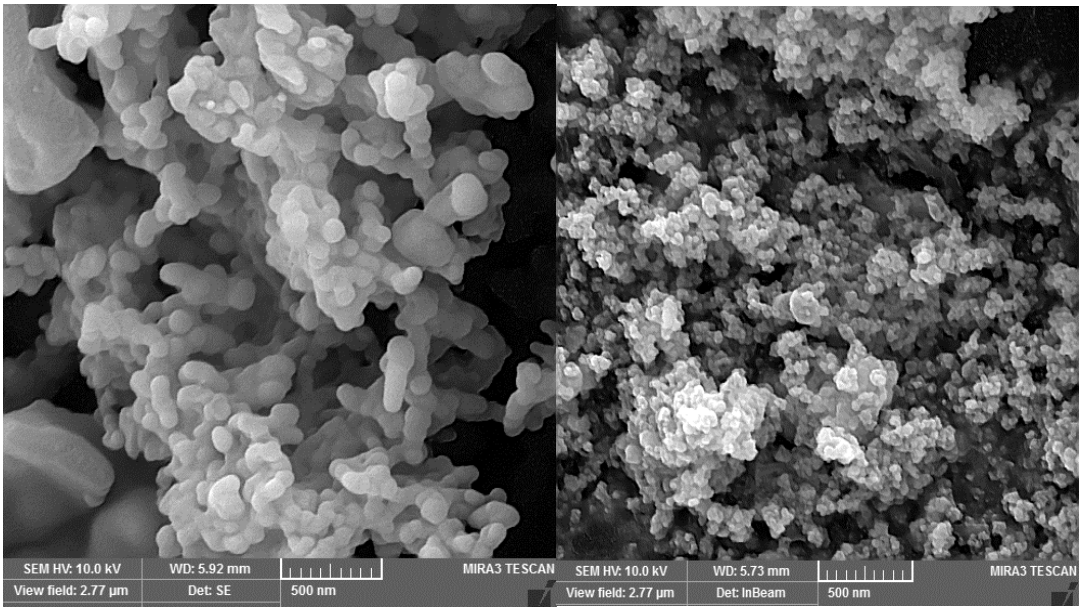


(a) (b)

**Fig. 3. FESEM images of the synthesized $Mn_2O_3$ (a) and $Mn_2O_3$-CuO nanocomposite (b)**

Additionally, the EDX spectrum of the manufactured $Mn_2O_3$-CuO composite is demonstrated in Figure 4, the results show that copper peaks are present at 8.95, 8.04, and 0.93 keV, oxygen peaks are present at 0.52 keV, and manganese peaks are present at 5.89 and 0.63 keV, which indicates that the composition of the manufactured $Mn_2O_3$-CuO composite contains these components. The lack of additional peaks in the EDX spectrum also suggests that the composed nanocomposite is highly pure.

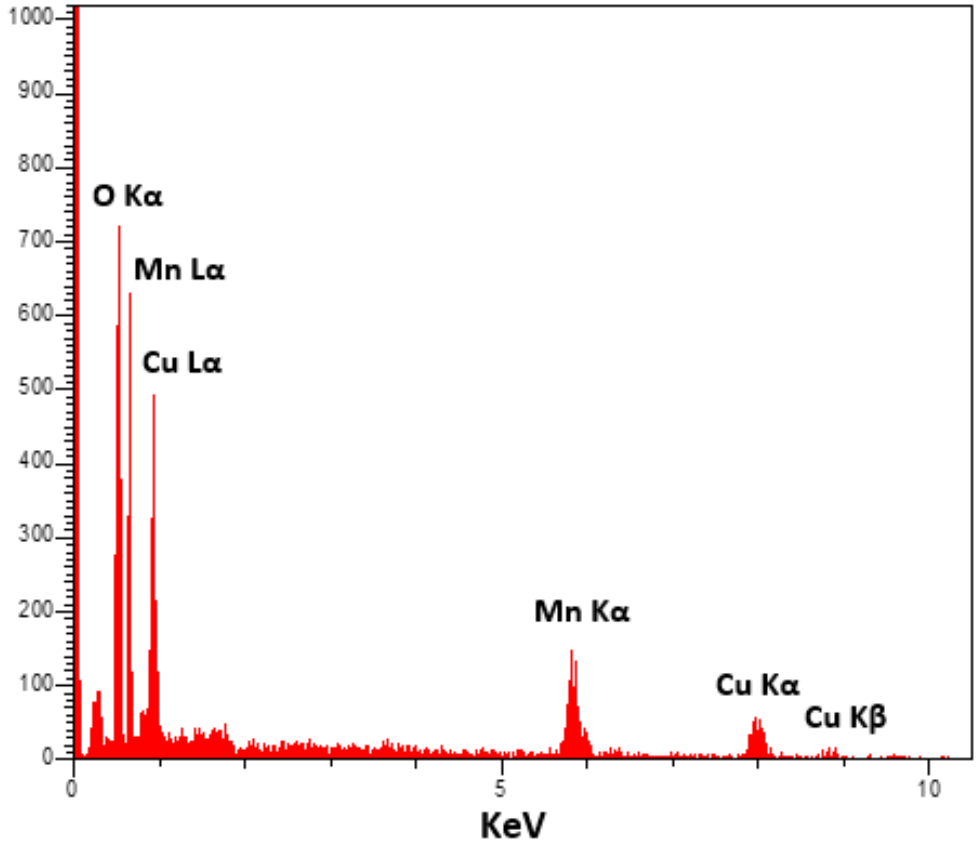


**Fig. 4. EDX spectrum of the synthesized $Mn_2O_3$-CuO nanocomposite**

### 3.2. Effect of pH

To examine the effect of pH on the effectiveness of RB5, the pH of solutions in the range of 3-9 was examined. As demonstrated in Figure 5, the removal efficiency decreased at alkaline pHs due to the repulsion between the like charges of the nanocomposite and the RB5, this is consistent with the pHZPC results ( Figure 6). The results demonstrated that the efficiency of the dye in the removal of the acidic and basic groups was the greatest at pH 5-6, and the removal efficiency was around 91% at pH 5. Additionally, at acidic pHs (pHs < 4), the decrease in efficiency of removal can be attributed to the neutralization of the charge on the surface of RB5, as well as the decreased rate of diffusion of RB5 to the surface of the $Mn_2O_3$-CuO composite. As a result, pH 5 was chosen as the most effective value in this research.

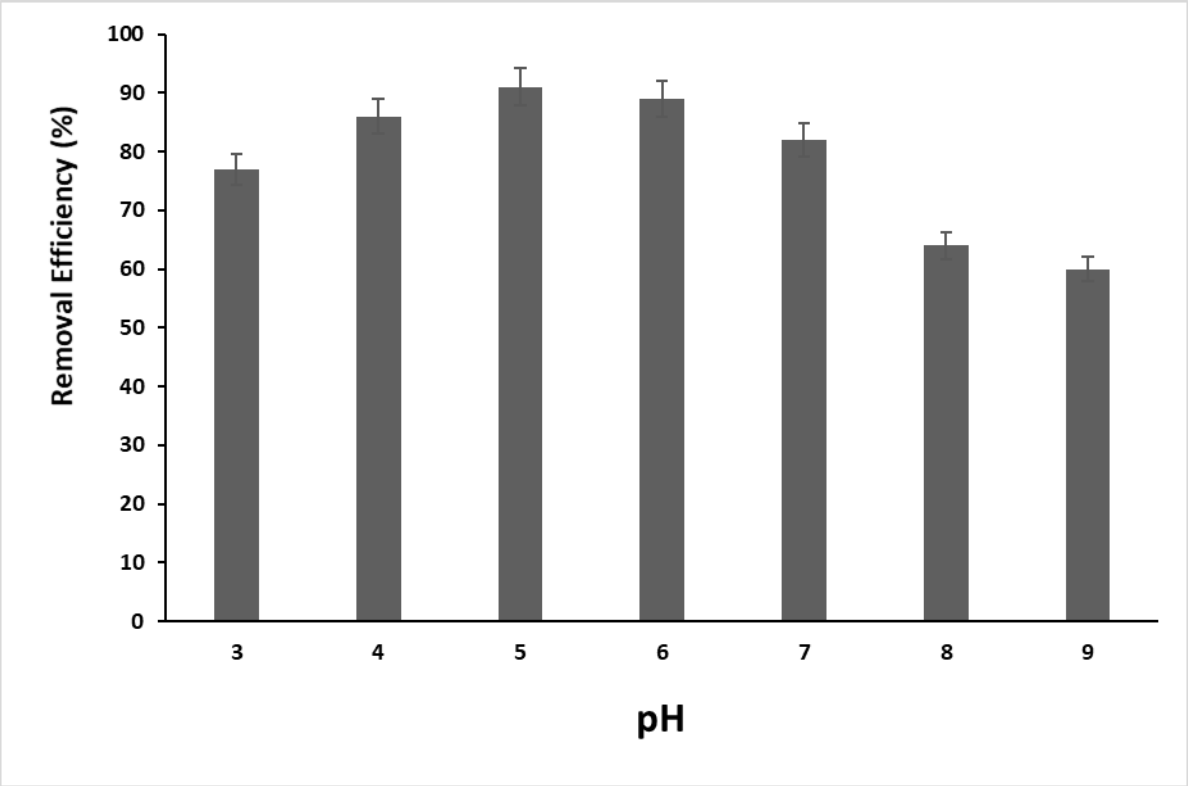


**Fig. 5. Effect of pH on the removal efficiency of RB5 dye. Conditions: 10 mg/L RB5, 40 mg $Mn_2O_3$-CuO nanocomposite and t=120 minutes.**

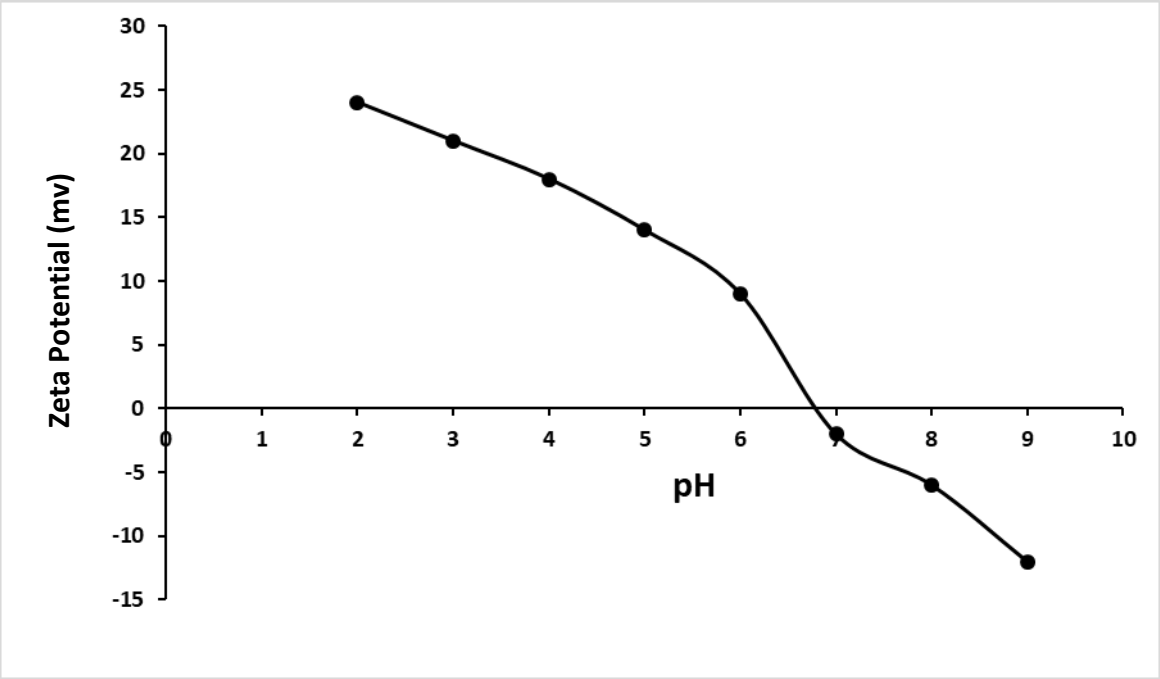


**Fig. 6. Zeta potential results for $Mn_2O_3$-CuO nanocomposite**

### 3.3. Photocatalyst Dosage

To study the effect of the amount of photocatalyst in the samples on the removal of the dye RB5, different amounts of photocatalyst were added to the samples ranging from 10 to 50 mg as shown in Figure 7. It was observed that the removal efficiency increased from about 39% to 92% as the amount of $Mn_2O_3$-CuO increased from 10 to 40 mg, and then decreased marginally. The increase in the volume of nanomaterials led to an increase in the efficiency of removal because of the increase in the number of active sites and enhanced photodegradation. However, the decrease in removal efficiency at higher concentrations of nanoparticles (50 mg) may be attributed to the increase in solution turbidity, which decreases the transmission of light. As a result, 40 mg of $Mn_2O_3$-CuO composite was considered the most effective dosage in this investigation.

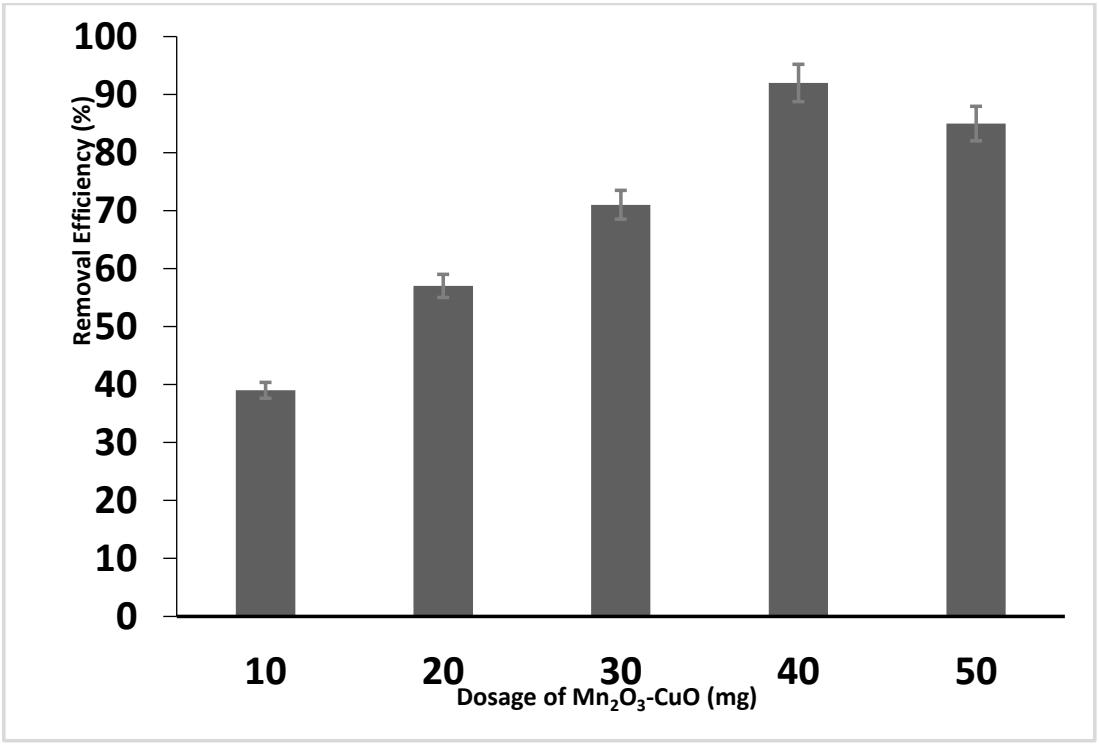


**Fig. 7. Effect of photocatalyst dosage on the removal efficiency of RB5 dye. Conditions: 10 mg/L RB5, pH=5 and t=120 minutes.**

### 3.4. Effect of initial concentration of dye

Figure 8a illustrates the effect of the initial concentration of dyes (10, 20, and 30 mg/l) on the rate of photodegradation. The results indicate that over 90% of the dye can be removable in 120 minutes. Conversely, the efficiency of photocatalytic removal decreases as the concentration of the dye increases over a given period of time, this may be due to the filling of active sites by the dye molecules. Figure 8b also demonstrates that the chemical mechanism of RB5 photodegradation follows the first-order model of chemical kinetics (Equation 2).

$$Ln(C_t/C_0) = -k_1 t$$

**Equation 2**

In Formula 2, the parameter $K_1$ is the rate constant (min-1), and its values for different concentrations of RhB are listed in Table 1. It's apparent that the initial amount of the adsorbate has an effect on the reaction rate, as a result, the pollutant's concentration increases, the degradation rate decreases.

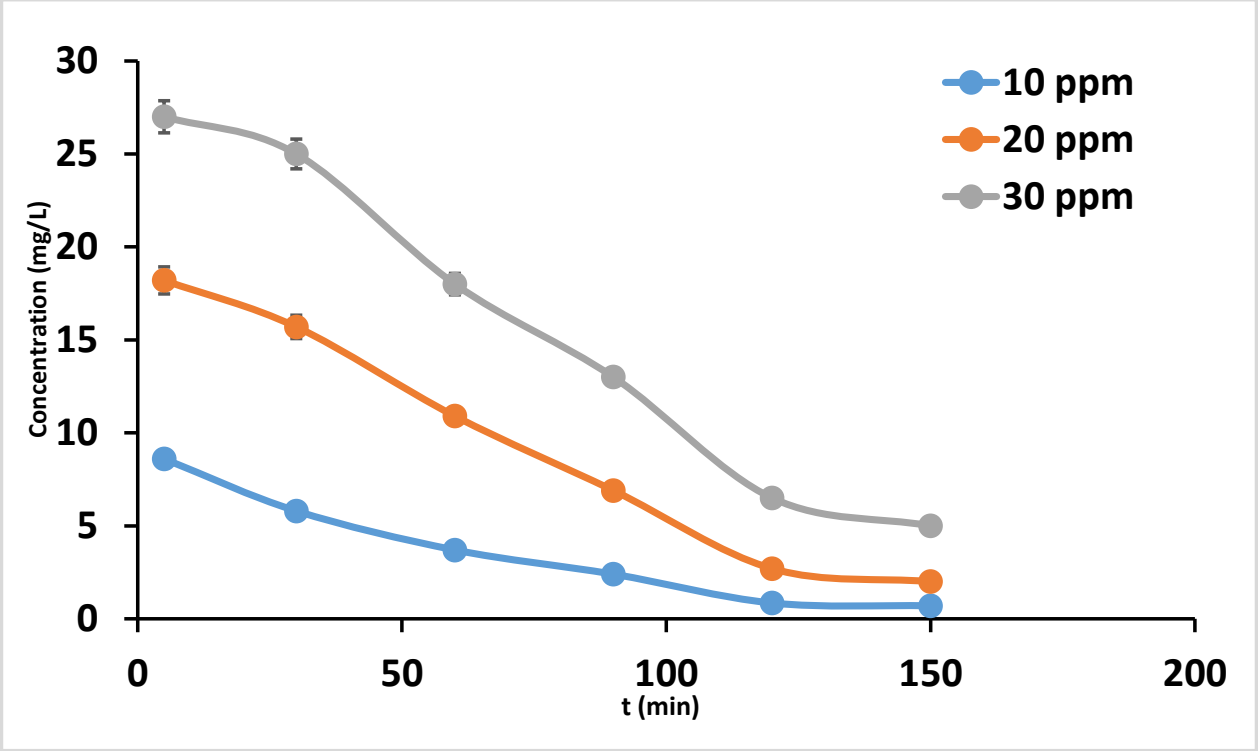


Ln Ct/C0

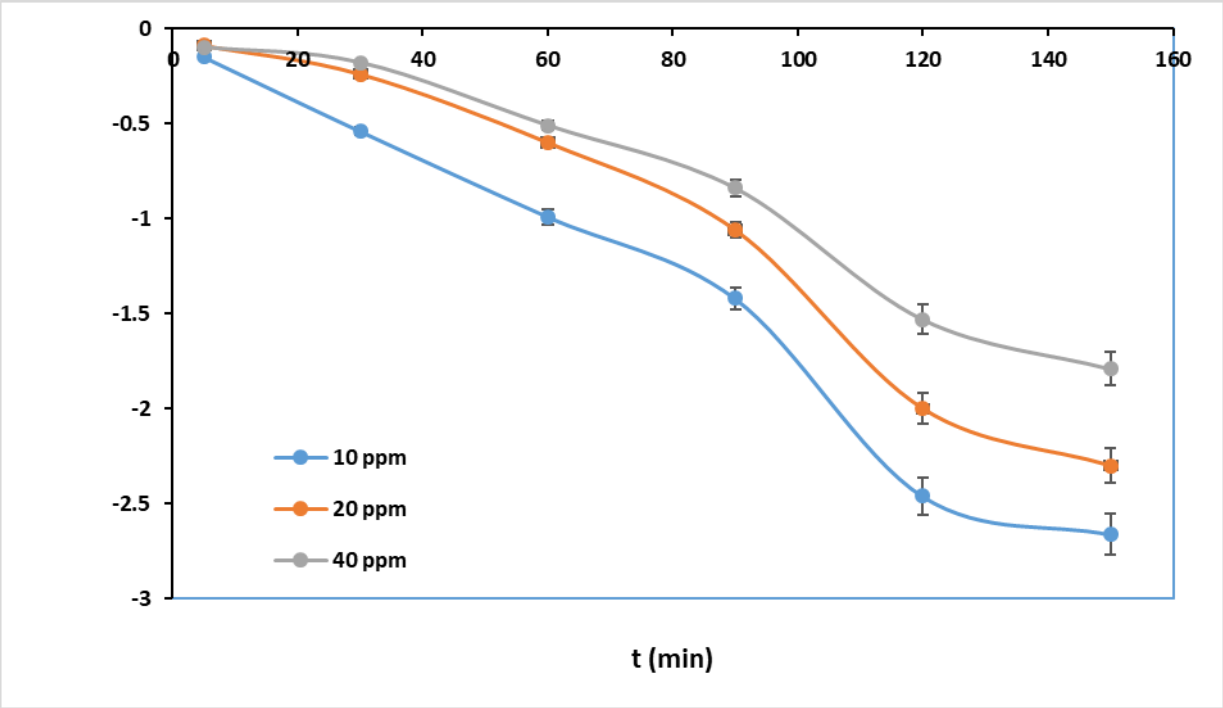


**Fig. 8. (a) The effect of initial RB5 concentration on the rate of dye degradation. (b) Pseudo-first-order reaction for RB5 degradation by $Mn_2O_3$-CuO nanocomposite (pH = 5, m=40 mg)**

**Table 1. Rate constants for $Mn_2O_3$-CuO nanocomposite at different concentration of RB5 (pH = 5, m = 40 mg)**

| $C_o$ (mg/L) | 10 | 20 | 40 |
|---|---|---|---|
| $K_1$ ($min^{-1}$) | 0.0183 | 0.0164 | 0.0126 |
| $R^2$ | 0.97 | 0.95 | 0.96 |

### 3.5. Reusability

To assess the recyclability of the generated photocatalyst for the removal of RB5, the MnO 3-CuO composite was evaluated for five cycles of photocatalytic degradation (see Figure 9). The efficiency of the photocatalytic process for the Mn2O 3 -CuO composite remained mostly unchanged after four cycles, this indicates that the composite can be repeated multiple times to remove the photocatalytic dye RB5. However, the decrease in the fifth cycle may be attributed to the filling of the active sites of the nanomaterials with the analytes.

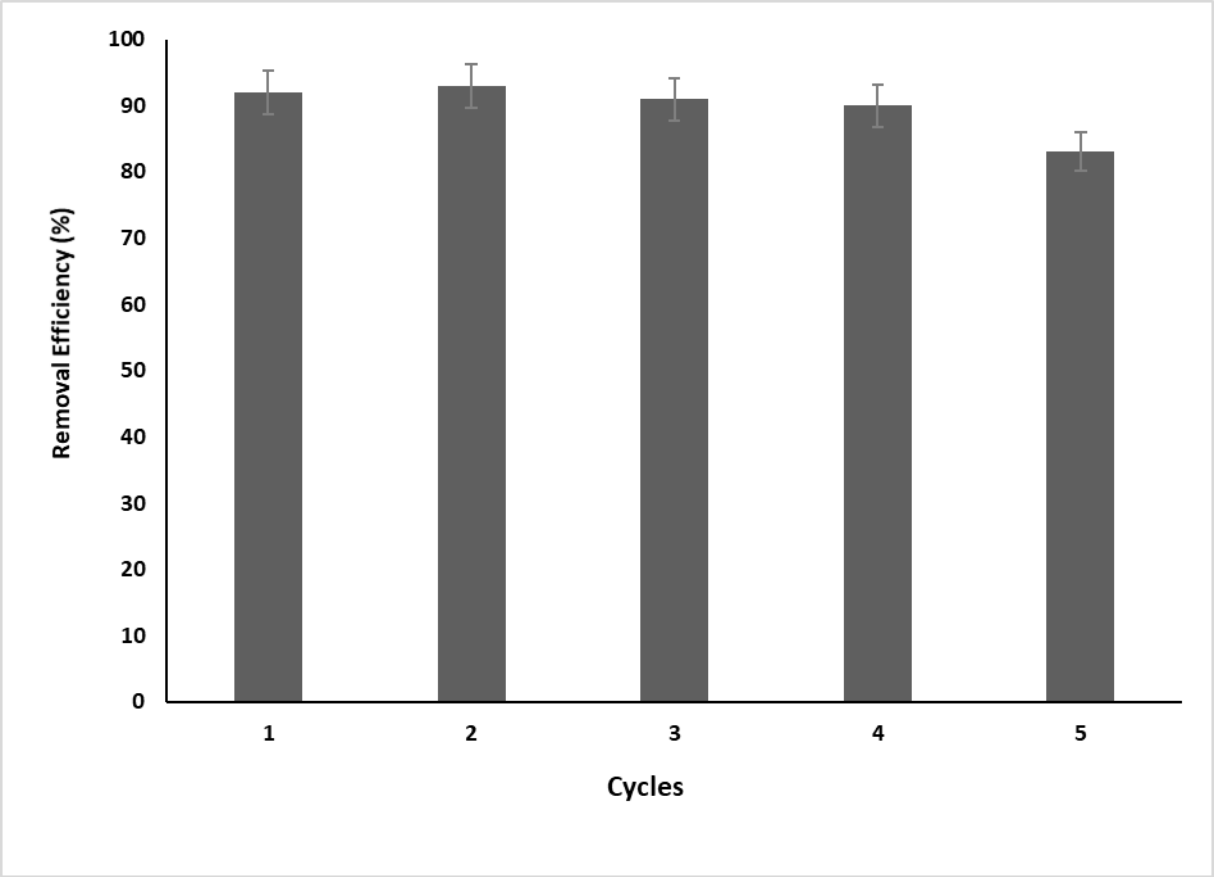


**Fig. 9. The reusability of $Mn_2O_3$-CuO nanocomposite photocatalysts in consecutive cycles (pH = 5, m= 40 mg, t = 120 min)**

## 4. Conclusion

In this study, Spirulina was used as a green extract and a green method was used to successfully synthesize Mn2O3-CuO nanocomposite. After characterization by FESEM, EDX, and XRD analysis, it was used as a photocatalyst for the degradation of dye RB5. By optimizing the parameters affecting the removal efficiency, it was found that when the pH value was 5 and the adsorbent dosage was 40 mg, more than 90% of the dye RB5 could be removed within 120 minutes under visible light irradiation. According to the results of this study, Mn2O3-CuO nanocomposite can be successfully used to remove dye RB5 from water samples.

## References

1. S. Benkhaya, S. M' rabet, A. El Harfi, A review on classifications, recent synthesis and applications of textile dyes. Inorg. Chem. Commun. 115 (2020) 107891.
2. R. Repon, B. Dev, A. Rahman, S. Jurkonienė, A. Haji, A. Alim, E. Kumpikaitė, Textile dyeing using natural mordants and dyes: a review. Environ. Chem. Lett. 22 (2024) 1473–1520.
3. K.T. Chung, Azo dyes and human health: A review. J Environ Sci Health C Environ Carcinog Ecotoxicol Rev. 34 (2016) 233-261.
4. B. Lellis, C.Z. Fávaro-Polonio, J.A. Pamphile, J. Cesar Polonio, Biotechnol. Res. Innov. 3 (2019) 275-290.
5. V. Ganthavee, A.P. Trzcinski, Removal of reactive black 5 in water using adsorption and electrochemical oxidation technology: kinetics, isotherms and mechanisms. Int. J. Environ. Sci. Technol. 22 (2025) 1083–1106.
6. R. Thapar Kapoor, M. Rafatullah, M.R. Siddiqui, M.A. Khan, M. Sillanpää, Removal of Reactive Black 5 Dye by Banana Peel Biochar and Evaluation of Its Phytotoxicity on Tomato. Sustainability 14 (2022) 4176.
7. M. Bhaumik, R.I. McCrindle, A. Maity, S. Agarwal, V. Kumar Gupta, Polyaniline nanofibers as highly effective re-usable adsorbent for removal of reactive black 5 from aqueous solutions. J. Colloid Interface Sci. 466 (2016) 442-451.
8. M. Chang, Y. Shih, Synthesis and application of magnetic iron oxide nanoparticles on the removal of Reactive Black 5: Reaction mechanism,

temperature and pH effects. J. Environ. Manag. 224 (2018) 235-242.

9. A. Nematollahzadeh, A. Shojaei, M. Karimi, Chemically modified organic/inorganic nanoporous composite particles for the adsorption of reactive black 5 from aqueous solution. React. Funct. Polym. 86 (2015) 7-15.
10. L. Semiz, Removal of reactive black 5 from wastewater by membrane filtration. Polym. Bull. 77 (2020) 3047–3059.
11. B. Dehingia, R. Lahkar, H. Kalita, Efficient removal of both cationic and anionic dyes from water using a single rGO/PSS nanocomposite membrane with superior permeability and high aqueous stability. J. Environ. Chem. Eng. 12 (2024) 112393.
12. T. Assefa Aragaw, A review of dye biodegradation in textile wastewater, challenges due to wastewater characteristics, and the potential of alkaliphiles. J. Hazard. Mater. Adv. 16 (2024) 100493.
13. Q. Wei, Y. Zhang, K. Zhang, J. Igadwa Mwasiagi, X. Zhao, C.W.K. Chow, R. Tang, Removal of direct dyes by coagulation: Adaptability and mechanism related to the molecular structure. Korean J. Chem. Eng. 39 (2022) 1850–1862.
14. S. Ihaddaden, D. Aberkane, A. Boukerroui, D. Robert, Removal of methylene blue (basic dye) by coagulation-flocculation with biomaterials (bentonite and Opuntia ficus indica). J. Water Process Eng. 49 (2022) 102952.
15. M. Saeed, M. Muneer, A.U. Haq, N. Akram, Photocatalysis: an effective tool for photodegradation of dyes—a review. Environ. Sci. Pollut. Res. 29 (2022) 293–311.
16. M. Rochkind, S. Pasternak, Y. Paz, Using Dyes for Evaluating Photocatalytic Properties: A Critical Review. Molecules 20 (2015) 88-110.
17. H. Saha, A. Dastider, J. Ferdous Anik, S. Rahman Mim, S. Talapatra, U. Das, M. Jamal, M. Billah, Photocatalytic performance of CuO NPs: An experimental approach for process parameter optimization for Rh B dye. Results Mater. 24 (2024) 100614.
18. P. Raizada, A. Sudhaik, S. Patial, V. Hasija, A.A. Parwaz Khan, P. Singh, S. Gautam, M. Kaur, V.H. Nguyen, Engineering nanostructures of CuO-based photocatalysts for water treatment: Current progress and future challenges. Arab. J. Chem. 13 (2020) 8424-8457.
19. T. Baran, A. Visibile, M. Busch, X. He, S. Wojtyla, S. Rondinini, A. Minguzzi, A. Vertova, Copper Oxide-Based Photocatalysts and Photocathodes: Fundamentals and Recent Advances. Molecules 26 (2021) 7271.
20. S. Naz, A. Gul, M. Zia, R. Javed, Synthesis, biomedical applications, and toxicity of CuO nanoparticles. Appl. Microbiol. Biotechnol.107 (2023) 1039–1061.
21. B. Maddiboyina, H. Krishna Vanamamalai, H. Roy, Ramaiah, S. Gandhi, M. Kavisri, M. Moovendhan, Food and drug industry applications of microalgae Spirulina platensis: A review. J. Basic Microbiol. 63 (2023) 573-583.
22. A. Harutyunyan, L. Gabrielyan, A. Aghajanyan, S. Gevorgyan, R. Schubert, C. Betzel, W. Kujawski, L. Gabrielyan, Comparative Study of Physicochemical Properties and Antibacterial Potential of Cyanobacteria Spirulina platensis-Derived and Chemically Synthesized Silver Nanoparticles. ACS Omega 9 (2024) 29410–29421.
23. M. Aamir, S. Hassan, A. Hamza Khan, M. Ibrar, S. Sarwar, K. Mahmood, N. Khan, D.A. Aljumaiah, A.H. Aldiaram, A.K. Alameer, A.J. Alsalman, A. Farid, Spirulina-mediated biosynthesis of gold nanoparticles: an interdisciplinary study on antimicrobial, antioxidant, and anticancer properties. J. Sol-Gel Sci. Technol. 113 (2025) 749–761.
24. R. Najjar, R. Awad, A. M. Abdel-Gaber, Physical Properties of Mn2O3 Nanoparticles Synthesized by Co-precipitation Method at Different pH Values. J. Supercond. Nov. Magn. 32 (2019) 885–892.
25. M.Y. Nassar, A.S. Amin, I.S. Ahmed, S. Abdallah, Sphere-like Mn2O3 nanoparticles: Facile hydrothermal synthesis and adsorption properties. J Taiwan Inst Chem Eng. 64 (2016) 79-88.
26. Alhalili, Z., Green synthesis of copper oxide nanoparticles CuO NPs from Eucalyptus Globoulus leaf extract: Adsorption and design of experiments. Arab. J. Chem. 15 (2022) 103739.
27. A. Bashiri Rezaie, M. Montazer, M. Mahmoudi Rad, environmentally friendly low-cost approach for nano copper oxide functionalization of cotton designed for antibacterial and photocatalytic applications. J. Clean. Prod. 204 (2018) 425-436.